Photonic band tuning in two-dimensional photonic crystal slab waveguides by atomic layer deposition

E. Graugnard, D. P. Gaillot, S. N. Dunham, C. W. Neff, T. Yamashita, and C. J. Summers[a)]
School of Materials Science and Engineering, Georgia Institute of Technology, Atlanta, Georgia 30332-0245

(Received 3 August 2006; accepted 22 August 2006; published online 31 October 2006)

The photonic bands of two-dimensional (2D) triangular lattice photonic crystal Si slab waveguides were statically tuned using low temperature atomic layer deposition (ALD) of TiO_2. Angular dependent reflectance measurements of bare and coated devices were well fitted by three-dimensional finite-difference time-domain calculations. The technique not only allows the physics of photonic band effects in 2D photonic crystals to be systematically studied but also demonstrates large static tuning and precise fine-scale control over band frequency and dispersion, with a frequency tuning range of 12% and precision of 0.005% per ALD cycle. Band tuning to achieve zero group velocity is demonstrated. © *2006 American Institute of Physics*.
[DOI: 10.1063/1.2360236]

Two-dimensional (2D) slab photonic crystals (PCs) are being actively investigated because of their many unique properties: submicron beam control,[1] self-collimation,[2] superprism effects,[3] negative refraction,[4] and the ability to control the speed of light.[5] All of these properties are dependent on the precise control of dielectric material, usually by electron-beam lithography, consisting of a periodic dielectric modulation with integrated line, point, and periodic defects.[6] Thus, the exact optical properties of the final 2D PC slab device are determined by the precision of the lithography process, with limited postfabrication tunability. Atomic layer deposition (ALD) has become a powerful tool for the fabrication of high quality three-dimensional PCs from both inorganic (opal) and organic (holographically patterned polymer) templates.[7,8] With ALD, highly conformal films can be grown with a precision of 0.05 nm, with a wide range of low temperature film growth protocols available.[9] Hence, ALD enables a high degree of control over material and structural properties, which allows for precise static tuning of optical properties.[10,11]

Here we report the application of ALD to 2D PC slab waveguides to tune precisely the photonic band frequencies and dispersion in as-fabricated devices. The photonic bands along high symmetry directions in a slab waveguide were measured using a resonant coupling technique[12,13] after conformally coating the slab with increasing thicknesses of TiO_2. The results demonstrate large ($\sim$12%) tuning in frequency of several of the photonic bands with a precision of $\sim$0.005%. The dispersion of the bands was also tuned by the film coating, with some bands changing from positive to negative slopes providing the ability to tune for a zero group velocity to enable ultraslow light propagation. This allows for precise postfabrication control of dielectric contrast within the device to tune precisely photonic band gap frequencies and the dispersion of bands used for negative refraction, selfcollimation, and slow light propagation phenomena.

A triangular lattice of air holes in a 300 nm thick single crystal silicon slab, shown in Fig. 1(a), was fabricated on a silicon-on-insulator substrate by electron-beam lithography and inductively coupled plasma etching. The lattice periodicity was 360 nm with a hole radius of 123 nm, as verified by scanning electron microscopy (SEM) images. Several unit cells of the as-fabricated device are shown in Fig. 1(a). Subsequently, the sample was conformally coated with amorphous TiO_2 (refractive index of 2.31 at 800 nm) by ALD. The depositions were performed at 100 °C in 20 nm steps (392 cycles at 0.051 nm/cycle) using $TiCl_4$ and H_2O precursors, as described in detail elsewhere.[7] A schematic cross section of the sample morphology for successive coatings is shown in Fig. 2. The effects of increasing conformal coating thickness are to reduce precisely and uniformly the diameter and the depth of the air holes. However, for an air-bridge-

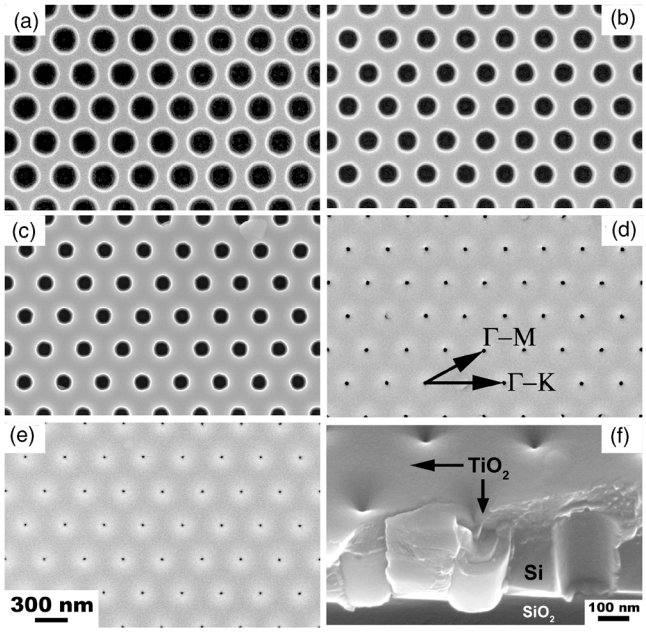

FIG. 1. Top-view scanning electron microscope images of a triangular lattice Si slab PC coated with TiO_2 ALD thicknesses of (a) 0 nm, (b) 20 nm, (c) 40 nm, (d) 90 nm, and (e) 120 nm. A cleaved cross section of the coated waveguide is shown in (f) and reveals complete infiltration of the air holes with solid TiO_2.

[a)]Electronic mail: chris.summers@mse.gatech.edu

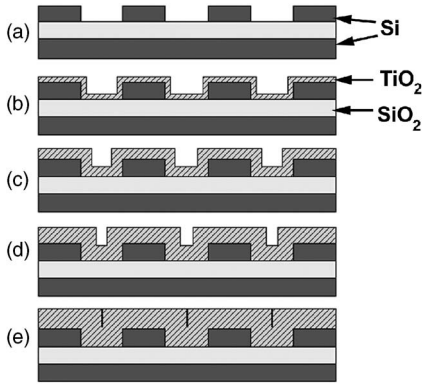

FIG. 2. Schematic of the cross section of the slab waveguide at each stage in the coating. The labels to the left of each stage refer to the labels in Fig. 1. Since the TiO_2 coatings are conformal, the holes fill from the bottom and the sides at an equal rate. In the final structure (e) the lattice has been completely filled with TiO_2 creating a slab cladding layer.

type slab waveguide, which has no underlying support layer, or in the case of very deep holes, the primary effect to the photonic band structure will be determined from the reduction in the air hole radius, which directly controls the air filling fraction. An additional effect is the overcoating of the slab, which becomes significant for thicker films. Depending on the dielectric constants of the slab and the ALD film, the overcoating layer will affect the confinement of light within the slab. In this case, the dielectric contrast between Si and TiO_2 is still quite high and a number of bands still exist below the light cone. Additionally, we note that this technique also serves as a template-patterning method for fabricating a TiO_2 PC slab device, which could be achieved by removing the Si slab layer. Such devices are interesting for applications operating at visible wavelengths.[14]

Figures 1(b)–1(e) show top-view SEM images of the sample coated with 20, 40, 90, and 120 nm of TiO_2, respectively. The crystal directions and magnification are the same for all images. The progressive and systematic reduction in the hole radii from ~123 to ~5 nm clearly confirms the uniformity and precision of the deposition and agrees well with the schematics shown in Fig. 2. The SEMs also reveal very little increase in the surface roughness from the ultrasmooth TiO_2 grown by low-temperature ALD. A cleaved cross section of the coated lattice is shown in Fig. 1(f), from which it can be seen that the air holes were completely filled with TiO_2.

The optical properties of the Si slab waveguide were characterized by resonant-coupling reflectance[12,13] along the main PC lattice symmetry directions, M-Γ and Γ-K, from 700 to 1700 nm. The measurement system consists of coaxial rotational stages to control the angles of incident and reflected light, which was routed to a long wavelength spectrometer equipped with an InGaAs photodiode. The slab waveguide device was optically probed before and after each deposition to monitor the progressive shifts in band structure. The data for the uncoated sample and after 40 and 120 nm TiO_2 coatings are shown in Fig. 3. Three-dimensional finite-difference time-domain (FDTD) calculations (solid lines in Fig. 3) were performed to model the coated device using a conformally defined slab dielectric function to represent accurately the TiO_2 coatings and the entire device. The FDTD data were observed to be in excellent agreement with the optical measurements for the lowest band and in very close

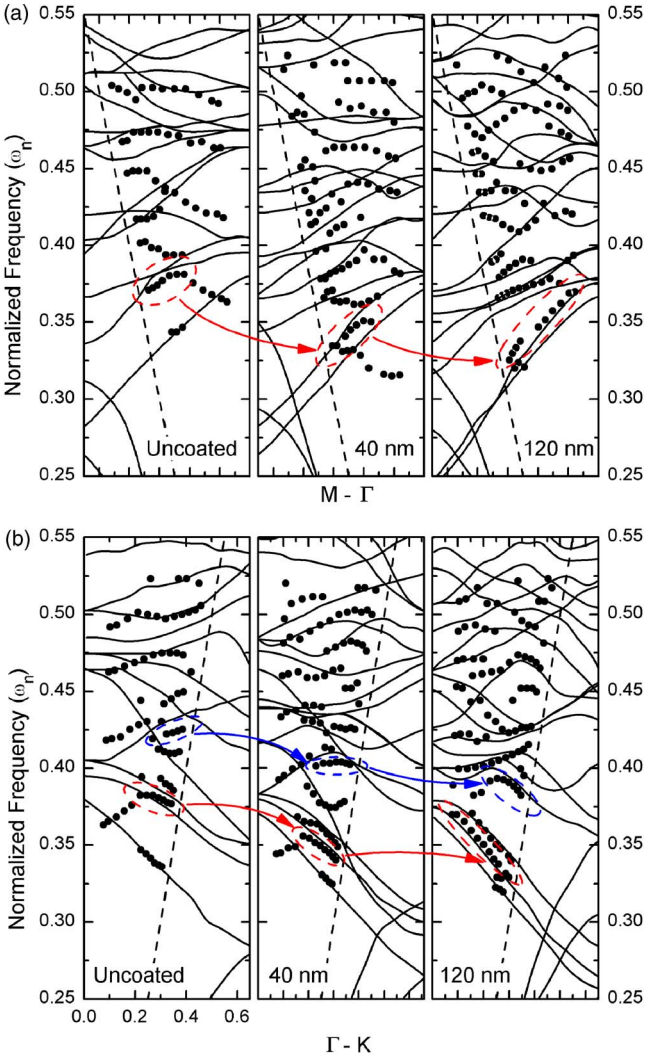

FIG. 3. (Color online) Measured (dots) and calculated (lines) photonic band structures for uncoated (left), 40 nm TiO_2 coated (center), and 120 nm coated (right) Si slab waveguide along the M-Γ (a) and Γ-K (b) directions. The dashed ellipses highlight the shifted bands.

agreement for all higher bands. The slight deviation of the high-order bands results from the wavelength dependence of the refractive indices for both Si and TiO_2, which was not included in the FDTD calculations. As expected, increased TiO_2 coatings shifted the bands to lower frequency as a consequence of increasing the average dielectric constant of the device by reducing the filling fraction of air. However, the data also revealed significant monotonic changes in the slope of several bands as the coating thickness increased. For the lowest measured band along the M-Γ direction and the second and fifth lowest bands along the Γ-K direction (indicated by the dashed ellipses), the midpoint frequency ($ka/2\pi = \sim 0.26$) and slope were measured and are plotted versus the TiO_2 coating thickness in Figs. 4(a) and 4(b), respectively. The midpoint of the M-Γ band was observed to shift from a normalized frequency ω_n of 0.380 to 0.334 for a 120 nm TiO_2 coating, indicating a shift of 12%. Since the TiO_2 film is deposited at 0.051 nm/ALD cycle, this enables a static tuning resolution of 0.005% per ALD cycle. Similar shifts and changes in dispersion for high order bands were observed along both high symmetry directions. For the Γ-K direction, the midpoint frequency of the second lowest band decreased by a similar amount (12% shift) from 0.382 to

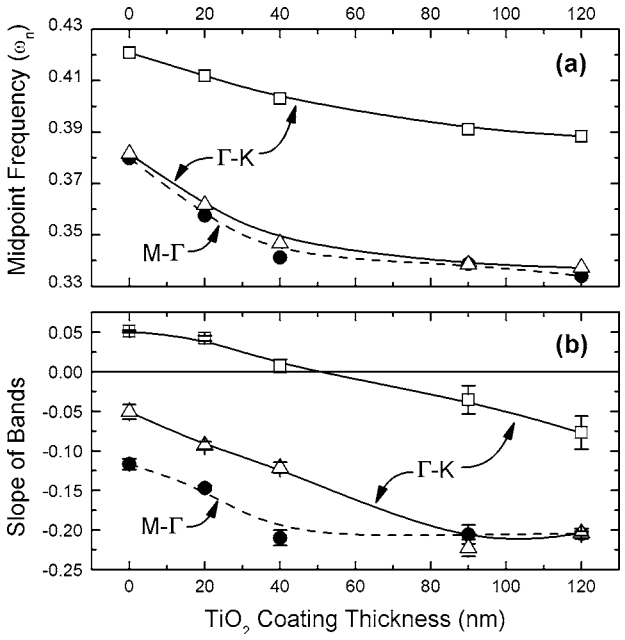

FIG. 4. Experimentally determined midpoint frequency (a) and slope (b) of the lowest order band along the M-Γ direction (solid circles) and the seconnd and fifth lowest bands along the Γ-K direction (open triangles and squares, respectively) as a function of TiO_2 thickness. Band midpoints were measured at a normalized k value of 0.26 for the lower bands and 0.30 for the high-order band. The x and y axes are the same for each panel set.

0.337. As shown in Fig. 4, the degree of band modification was observed to decrease as the air holes were filled with TiO_2, which can be understood in terms of the reduced fractional change in the dielectric contrast as the holes become filled. Changes in the air filling fraction had a larger effect initially as the holes were mostly air. For both directions, the slope of the bands increased with TiO_2 coating, although the slope along the Γ-K direction increased by a larger degree. Significantly, along the Γ-K direction, the band at $\omega_n = 0.423$ in the uncoated device (enclosed by the upper dashed blue ellipses) initially exhibited a positive slope. When coated with 40 nm of TiO_2, the band was shifted to lower frequency and the slope was reduced to almost zero. After 120 nm of TiO_2 the band was shifted further downwards, as expected, but the slope of the band was reversed and became negative. The data for the fifth band are plotted in Fig. 4(b) (open squares) and provide direct evidence of the ability to tune band dispersion to achieve zero group velocity and consequently enable ultraslow light propagation. Thus, these results directly demonstrate the capability of this technique to enable simultaneously very large static adjustments in the frequency and dispersion of the photonic band structure with extremely high precision. It follows that this powerful process, which can be applied to any 2D structure with a large number of coating materials, enables precise and reproducible control over the optical properties of photonic crystal devices.

In summary, we have demonstrated static photonic band tuning in a two-dimensional triangular lattice photonic crystal Si slab waveguide by nanoscale modification of the dielectric contrast using atomic layer deposition of TiO_2. For the case of a Si waveguide structure and TiO_2 deposition, a tuning range of 12% with a precision of 0.005% has been demonstrated in the optical properties and photonic band structure. Greater control and finer scale tuning can be achieved by depositing a film with a lower refractive index than TiO_2. Conversely, a larger range of frequency tuning can be achieved with higher index films, with the tuning precision determined by the deposition rate. It has been demonstrated that adjustments can be made not only to the band frequency but also to the dispersion, enabling precise tuning to achieve a zero group velocity for slow-light applications. The precision and uniform control of this technique enables unprecedented adjustment to the dispersion properties of any 2D photonic crystal. Additionally, by the application of multicomponent ALD, this technique facilitates the formation of layered and composite 2D PC waveguides thus opening new fabrication routes to control dispersion, propagation, and dielectric contrast. Also the technique can be used to add increased functionality and to fabricate active device structures for integration with electronic devices. This capability will enable structures to be tuned for specific purposes, such as beam guiding, dispersion, and slow light control, and may also impact the design of ultralow loss structures.

The authors thank V. Chawla for valuable assistance with this work. This work was supported by the U.S. Army Research Office under MURI Contract No. DAAD19-01-1-0603.

[1] S. J. McNab, N. Moll, and Y. A. Vlasov, Opt. Express **11**, 2927 (2003).
[2] H. Kosaka, T. Kawashima, A. Tomita, M. Notomi, T. Tamamura, T. Sato, and S. Kawakami, Appl. Phys. Lett. **74**, 1212 (1999).
[3] H. Kosaka, T. Kawashima, A. Tomita, M. Notomi, T. Tamamura, T. Sato, and S. Kawakami, Phys. Rev. B **58**, R10096 (1998).
[4] E. Schonbrun, T. Yamashita, W. Park, and C. J. Summers, Phys. Rev. B **73**, 195117 (2006).
[5] H. Gersen, T. J. Karle, R. J. P. Engelen, W. Bogaerts, J. P. Korterik, N. F. van Hulst, T. F. Krauss, and L. Kuipers, Phys. Rev. Lett. **94**, 073903 (2005).
[6] Z. Zhang and M. Qiu, Opt. Express **13**, 2596 (2005).
[7] J. S. King, E. Graugnard, and C. J. Summers, Adv. Mater. (Weinheim, Ger.) **17**, 1010 (2005).
[8] J. S. King, E. Graugnard, O. M. Roche, D. N. Sharp, J. Scrimgeour, R. G. Denning, A. J. Turberfield, and C. J. Summers, Adv. Mater. (Weinheim, Ger.) **18**, 1561 (2006).
[9] M. Ritala and A. Leskelä, in *Handbook of Thin Film Materials*, edited by H. S. Nalwa (Academic, San Diego, 2001), Vol. 1, 103–159.
[10] J. S. King, E. Graugnard, and C. J. Summers, Appl. Phys. Lett. **88**, 081109 (2006).
[11] E. Graugnard, J. S. King, D. P. Gaillot, and C. J. Summers, Adv. Funct. Mater. **16**, 1187 (2006).
[12] V. N. Astratov, D. M. Whittaker, I. S. Culshaw, R. M. Stevenson, M. S. Skolnick, T. F. Krauss, and R. M. De La Rue, Phys. Rev. B **60**, R16255 (1999).
[13] D. Coquillat, A. Ribayrol, R. M. D. L. Rue, M. L. V. d'Yerville, D. Cassagne, and J. P. Albert, Appl. Phys. B: Lasers Opt. **73**, 591 (2001).
[14] X. Wang, M. Fujimaki, and K. Awazu, Opt. Express **13**, 1486 (2005).